Gain-of-Function Phenotypes of Many *CLAVATA3/ESR* Genes, Including Four New Family Members, Correlate with Tandem Variations in the Conserved *CLAVATA3/ESR* Domain[1][W]

Timothy J. Strabala[2]*, Philip J. O'Donnell, Anne-Marie Smit[2], Charles Ampomah-Dwamena[3], E. Jane Martin, Natalie Netzler, Niels J. Nieuwenhuizen[3], Brian D. Quinn[3], Humphrey C.C. Foote[4], and Keith R. Hudson

AgriGenesis Biosciences Limited, Auckland, New Zealand

Secreted peptide ligands are known to play key roles in the regulation of plant growth, development, and environmental responses. However, phenotypes for surprisingly few such genes have been identified via loss-of-function mutant screens. To begin to understand the processes regulated by the *CLAVATA3* (*CLV3*)/*ESR* (*CLE*) ligand gene family, we took a systems approach to gene identification and gain-of-function phenotype screens in transgenic plants. We identified four new *CLE* family members in the Arabidopsis (*Arabidopsis thaliana*) genome sequence and determined their relative transcript levels in various organs. Overexpression of *CLV3* and the 17 *CLE* genes we tested resulted in premature mortality and/or developmental timing delays in transgenic Arabidopsis plants. Overexpression of 10 *CLE* genes and the *CLV3* positive control resulted in arrest of growth from the shoot apical meristem (SAM). Overexpression of nearly all the *CLE* genes and *CLV3* resulted in either inhibition or stimulation of root growth. *CLE4* expression reversed the SAM proliferation phenotype of a *clv3* mutant to one of SAM arrest. Dwarf plants resulted from overexpression of five *CLE* genes. Overexpression of new family members *CLE42* and *CLE44* resulted in distinctive shrub-like dwarf plants lacking apical dominance. Our results indicate the capacity for functional redundancy of many of the CLE ligands. Additionally, overexpression phenotypes of various *CLE* family members suggest roles in organ size regulation, apical dominance, and root growth. Similarities among overexpression phenotypes of many *CLE* genes correlate with similarities in their CLE domain sequences, suggesting that the CLE domain is responsible for interaction with cognate receptors.

Since the discovery of systemin, the first plant peptide ligand (Pearce et al., 1991), proteinaceous ligands have been demonstrated to play diverse roles in plant growth, development, and responses to environmental stimuli (Pearce et al., 2001; for review, see Lindsey et al., 2002), including phenomena such as self-incompatibility (SCR), wounding responses (systemin), cell division (phytosulfokine), root growth (RALF), floral abscission (IDA), and maintenance of the shoot apical meristem (SAM;CLAVATA3 [CLV3]). These ligands are all members of gene families (Cock and McCormick, 2001; Vanoosthuyse et al., 2001; Yang et al., 2001; Olsen et al., 2002; Butenko et al., 2003; Haruta and Constabel, 2003; Ryan and Pearce, 2003). These gene families have been defined based on amino acid sequence similarity, with the exception of the systemin family, whose members are functionally defined by their biochemically demonstrated roles in systemic wound responses (Ryan and Pearce, 2003). Although the biological functions of the archetypal members of these gene families are known, little is known about the roles that most of the other members of these families play in plants.

Members of the *CLV3/ESR* (*CLE*) gene family have been found in many angiosperm species (Cock and McCormick, 2001). With at least 27 members in Arabidopsis (*Arabidopsis thaliana*), the *CLE* genes constitute one of the larger peptide ligand families (Cock and McCormick, 2001; Haas et al., 2002; Sharma et al., 2003b). All but one of the Arabidopsis *CLE* genes are known to be transcribed (Sharma et al., 2003b). The *ESR* members of the family are found in the embryo-surrounding region in developing maize (*Zea mays*) seeds (Bonello et al., 2000). ESR proteins are secreted and interact with an unidentified 35-kD protein (Bonello et al., 2000, 2002).

The best understood of the CLE proteins is the ligand CLV3, encoded by the archetypal member of the *CLE*

[1] This work was supported in part by the Foundation for Research, Science and Technology (NZ; grant no. GENX0201).

[2] Present address: Scion (the trading name for New Zealand Forest Research Institute Ltd.), Sala Street, Private Bag 3020, Rotorua, New Zealand.

[3] Present address: HortResearch, 120 Mt. Albert Road, Private Bag 92 169, Auckland, New Zealand.

[4] Present address: AJ Park, P.O. Box 949, Wellington, New Zealand.

* Corresponding author; e-mail tim.strabala@scionresearch.com; fax 64–7–343–5444.

The author responsible for distribution of materials integral to the findings presented in this article in accordance with the policy described in the Instructions for Authors (www.plantphysiol.org) is: Timothy J. Strabala (tim.strabala@scionresearch.com).

[W] The online version of this article contains Web-only data.

Article, publication date, and citation information can be found at www.plantphysiol.org/cgi/doi/10.1104/pp.105.075515.

gene family (Fletcher et al., 1999; Cock and McCormick, 2001). The *clv3* mutants are characterized by the expansion of the SAM, fasciation of stems and leaves, and supernumerary floral organs (Clark et al., 1995). In contrast, overexpression of *CLV3* results in plants in which the SAM is not maintained and organogenesis from the shoot tip is thereby arrested (Brand et al., 2000). *CLV3* is expressed in the tunica layers of the dome of the SAM (Fletcher et al., 1999). The CLV3 protein is secreted and interacts directly with the CLV1/CLV2 receptor complex in the central region of the corpus (Rojo et al., 2002). Together, these three proteins act to regulate the size of the SAM by down-regulating the expression of the transcription factor WUSCHEL (WUS). WUS in turn up-regulates meristem cell formation and *CLV3* expression, resulting in a dynamic feedback loop with the CLV complex (Brand et al., 2000; for review, see Bäurle and Laux, 2003; Carles and Fletcher, 2003; Sharma et al., 2003a). Mutants in the *wus* gene display arrest of growth from the SAM, followed by resumption of growth from axillary buds in a stop-start fashion (Laux et al., 1996), a phenotype similar to weak-to-moderate overexpressers of *CLV3* (Brand et al., 2000).

Developmental roles are suggested for some of the other CLE proteins. Expression of *CLE40* under the control of the *CLV3* promoter complements the *clv3* mutant phenotype, demonstrating the capacity for functional redundancy between these two genes (Hobe et al., 2003). However, actual functional redundancy between CLV3 and CLE40 does not appear to occur in nature because a *cle40-En* insertional mutation has no apparent effect on SAM maintenance, but rather causes alterations in root growth (Hobe et al., 2003). Also suggesting the involvement of a *CLE* gene or genes in root developmental processes, overexpression of Arabidopsis *CLE19* with a root-specific promoter (Casamitjana-Martinez et al., 2003) or the rapeseed (*Brassica napus*) *BnCLE19* gene with a constitutive promoter (Fiers et al., 2004) alters root growth and development. It seems unlikely that CLE19 or BnCLE19 act solely in root development because *BnCLE19* is strongly expressed in cotyledon anlagen in embryos, in the abaxial portions of leaf anlagen, and at the site of presumptive pistil formation in developing flowers in mature plants (Fiers et al., 2004).

Although the loss-of-function approach to genetics is an extremely powerful tool in the identification of gene function, functional redundancy of genes can complicate this approach in some instances, at least in plants (Alonso et al., 2003; discussed in Zhang, 2003). In the case of the *CLE* family, it was recently shown that Arabidopsis *CLE19* insertional mutant lines failed to yield phenotypes, suggesting the possibility of a functionally redundant partner or partners to this gene (Fiers et al., 2004). Additionally, the short physical lengths of many genes, such as those encoding peptide ligands, decrease the likelihood of generating mutations in such loci. The complementary approach, gain-of-function analysis, has been applied successfully in plants via activation-tagging screens (e.g. Kakimoto, 1996; Kirch et al., 2003; Wen et al., 2004). Expressed sequence tag (EST) and genome databases have allowed systematic, gene sequence-based gain-of-function screens to be applied comprehensively to the analysis of gene function (Stevenson et al., 2001). In Arabidopsis, sequence-based gain-of-function approaches have led to significant improvements in knowledge regarding the roles of transcription factors in growth, development, disease resistance, and other phenomena. In particular, overexpression approaches to assess gene function have yielded useful insights in many cases where loss-of-function approaches have not (for review, see Zhang, 2003).

Correct identification and annotation of genes in genome sequences is incomplete and much effort is being invested in methods to improve gene identification (Haas et al., 2002). Again, the short lengths of ligand gene sequences, combined with limited regions of similarity among members of a family, such as the *CLE* family, make difficult the comprehensive identification of all members of a gene family. Therefore, we took a systems-based approach to gene identification and gene overexpression to identify function for the members of peptide ligand gene families from Arabidopsis and other species (Grigor et al., 2003).

We identified four previously unannotated *CLE* family members in the Arabidopsis genome sequence. Three of these genes appear to constitute a new clade on the CLE family phylogenetic tree, grouping with another recently identified *CLE* gene, *CLE41* (Haas et al., 2002). We overexpressed *CLV3* and 17 Arabidopsis L. Heynh. cv Columbia (Col-0) *CLE* genes in Arabidopsis. The resulting phenotypes we observed can be categorized into four partially overlapping classes: (1) phenotypes similar to *wus* mutants and plants overexpressing *CLV3* (the *wus*-like phenotype); (2) dwarf growth habit, often accompanied by anthocyanin overproduction; (3) a novel shrub-like phenotype characterized by dwarf growth habit accompanied by a lack of apical dominance; and (4) stimulation of root elongation. Additionally, overexpression of all the *CLE* genes we tested resulted in developmental timing delays relative to wild-type controls. Two of the three new *CLE* family members we tested displayed the shrub-like phenotype. The *wus*-like phenotypes and the shrub-like phenotypes strongly correlated with the sequences of the family-defining 14-amino acid C-terminal CLE domains in the transgenes, suggesting that the CLE domain determines the overexpression phenotype. Furthermore, these results suggest that genes within these classes interact with similar receptors and/or play functionally redundant roles in Arabidopsis, likely in developmental processes other than SAM homeostasis.

RESULTS

Identification of Novel *CLE* Family Members and Phylogenetic Analysis of the *CLE* Family

The central role played by CLV3 in SAM homeostasis led us to systematically investigate the functional roles taken by other *CLE* gene family members in

Arabidopsis. Therefore, we searched the Arabidopsis genome sequence for possible genes related to *CLV3*. This search resulted in the identification of four novel family members in addition to the known *CLE* gene family members (Cock and McCormick, 2001; Sharma et al., 2003b). We named these family members *CLE42*, *43*, *44*, and *45* in keeping with the existing *CLE* gene nomenclature (Fig. 1A). We also identified another *CLE* family member, *CLE41*, the predicted protein sequence of which is most similar to CLE42 and CLE44 (Fig. 1A). *CLE41*, *43*, and *44* are found in GenBank as cDNA clones (Supplemental Table I). Of these cDNA clones, only *CLE41* has been identified as a *CLE* family member (Haas et al., 2002). This gene was annotated as part of an EST-assisted genome annotation effort, along with *CLE44*, which was annotated as an unidentified full-length EST clone (Haas et al., 2002). *CLE43* has been annotated as an unidentified silique EST (Supplemental Table I). None of these genes has otherwise been described. Like most members of the *CLE* family, none of these new genes contain introns (data not shown). Furthermore, analysis of the predicted protein sequences of *CLE41* to *45* suggests that these are all secreted proteins, with signal peptides as predicted by SignalP (Nielsen et al., 1997; Fig. 1A).

As has been noted previously (Sharma et al., 2003b), there is little sequence conservation among the *CLE* genes, other than the CLE domain itself. Including the newly identified family members, the consensus sequence of the CLE domain is SKRLVPSGPNPLHN (Fig. 2). None of the predicted consensus amino acid residues is absolutely conserved throughout the gene family. However, predicted amino acids at positions 3, 8, 9, 10, 11, and 13 (numbering as in Fig. 2) are conserved in >90% of the CLE domain sequences. Of the 31 family members, CLE9 and CLE10 most closely match the consensus, differing only at relatively degenerate position 1 (Fig. 2). CLE7 least resembles the consensus CLE domain, with eight differences from

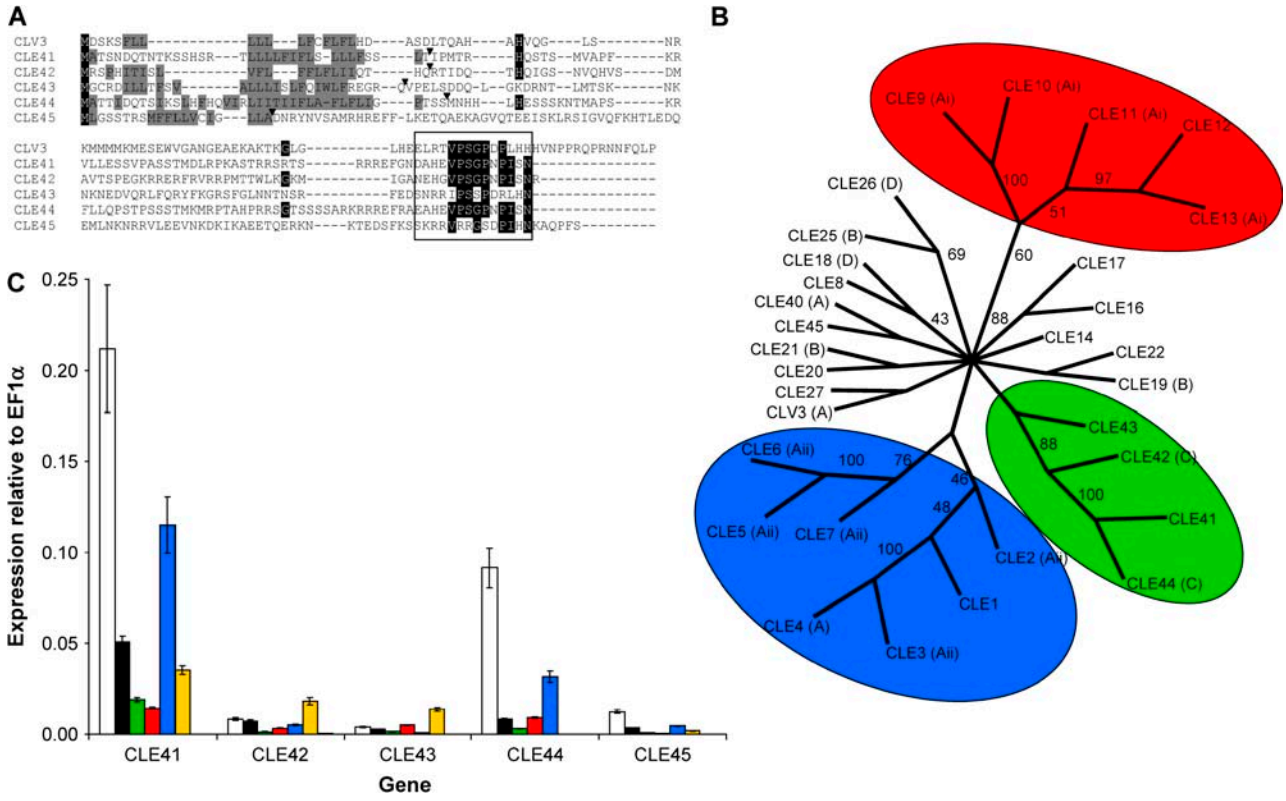

Figure 1. Predicted amino acid sequences, tissue specificity of expression, and phylogenetic analysis of the Arabidopsis *CLE41* to *45* genes in relation to the other *CLE* family members. A, Conceptual protein sequences of *CLE41* to *45* and the archetype *CLV3* gene were aligned using ClustalX (Thompson et al., 1997). Amino acid residues that are identical in at least four of the predicted protein sequences are highlighted in black. Hydrophobic amino acids in the predicted signal peptides are highlighted in gray. Predicted signal peptide cleavage sites for CLE41 to 45 are denoted by arrowheads. The CLE domain sequences are boxed. B, PAUP* 4.0 analysis of the CLE family predicted protein sequences. Bootstrap values of 40% and above from the neighbor-joining analysis of the predicted amino acid sequences of the *CLE* genes are shown at the appropriate nodes of the unrooted phylogenetic tree. The overexpression phenotypic classification (where known) as described in Figure 2 appears next to the name of the gene. The major phylogenetic groupings are all emphasized by red, blue, and green ovals behind the branches. C, Expression levels of *CLE41* to *45* relative to an elongation factor 1α control. White bars, Inflorescence stems; black bars, unopened flowers; green bars, developing siliques; red bars, rosette leaves; blue bars, roots; gold bars, seedlings.

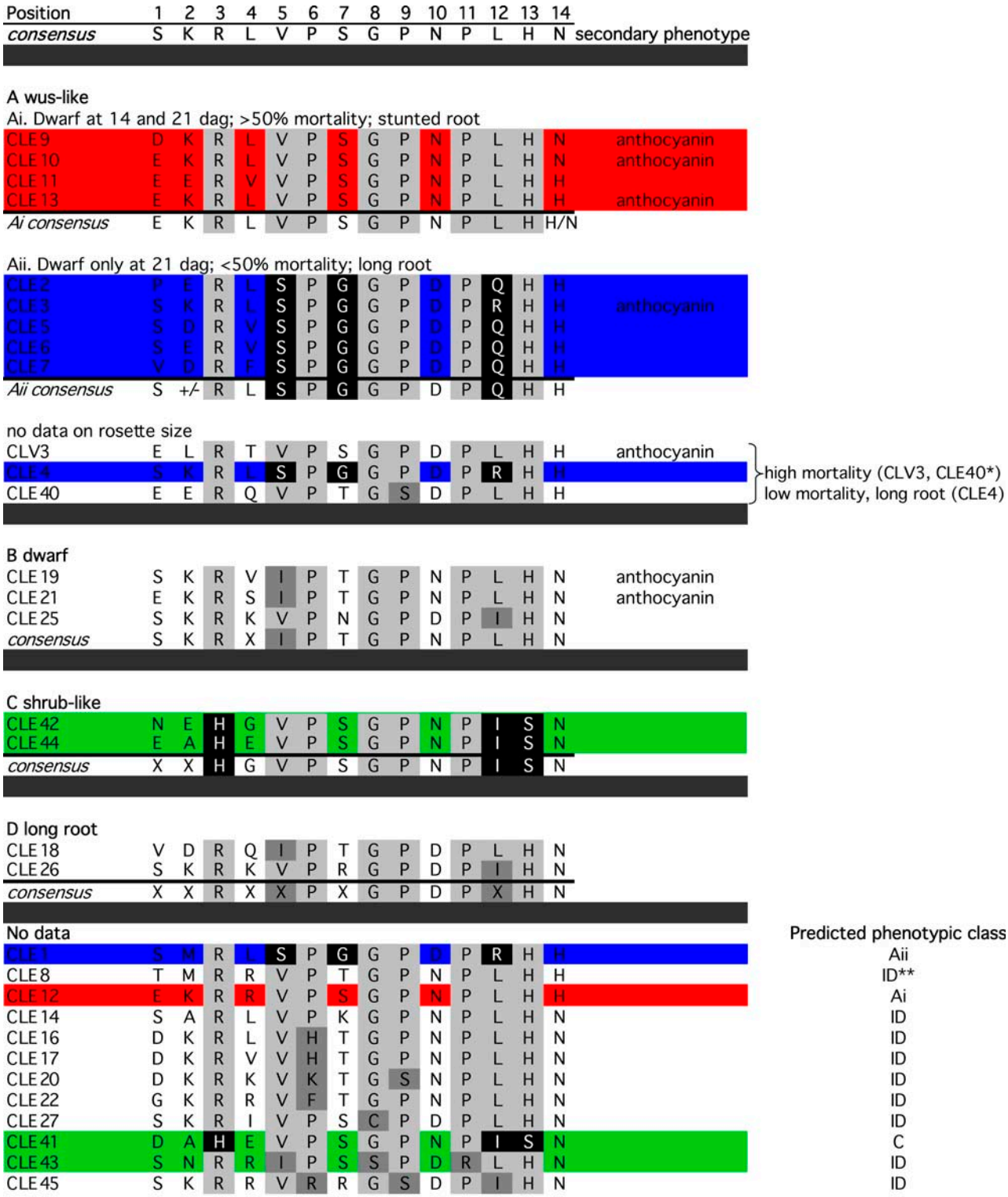

Figure 2. Comparison of the predicted CLE domains of the Arabidopsis *CLE* genes. The predicted protein CLE domains of the Arabidopsis *CLE* family members are aligned. Amino acid numbering of the CLE domain appears at the top. A consensus sequence of all the CLE domains is shown below the amino acid numbering. A, CLE domain sequences of the *CLE* genes that cause the *wus*-like phenotype. Ai, CLE domain sequences of the *wus*-like CLE genes that showed dwarfing only at 21 d DAG,

the consensus (Fig. 2). The conceptual CLE41 to 45 proteins are found within these extremes of divergence from the CLE domain consensus. Only CLE41, 42, and 44 differ from the consensus at positions 3 and 13, with His in place of Arg at position 3 and Asn in place of His at position 13 (Fig. 2). Despite their divergence from two of the best-conserved amino acids in the CLE domain, CLE41, 42, and 44 all have an uninterrupted core of seven conserved amino acids (positions 5–11) and are less divergent from the main consensus than CLE7. The predicted CLE43 protein also diverges from the consensus at the otherwise perfectly conserved Pro residue at position 11 with an Arg residue, but is nonetheless a good match to the main consensus. The predicted CLE45 is one of only three predicted proteins that diverge at position 9, substituting a Pro with a Ser, but the same substitution is also found in CLE20 and CLE40.

We examined the phylogenetic relationship of the new putative CLE family members to the rest of the CLE proteins. Like Sharma et al. (2003b), we observed that the predicted CLE1 to 7 proteins all group in a single clade and that the CLE3/4 and CLE5/6 pairs both group with 100% bootstrap values in a 1,000-iteration neighbor-joining analysis (Fig. 1B). Unlike Sharma et al. (2003b), our analysis grouped CLE9 to 13 in a single clade, with a bootstrap value of 60% (Fig. 1B). Bootstrap values of 100% and 97% were generated for the CLE9/10 and CLE12/13 pairs, respectively (Fig. 1B). Our analysis also grouped the conceptual CLE41, 42, 43, and 44 proteins in a single new clade (Fig. 1B). The strongest relationship was suggested for CLE41, 42, and 44, with bootstrap values of 88% for these three predicted proteins and 100% for the CLE41/CLE44 pair (Fig. 1B).

To determine whether the four newly identified *CLE* gene family members and *CLE41* were expressed genes, we conducted real-time PCR experiments with gene-specific primers for *CLE41* to *45*. We also examined the tissue and organ specificity of expression of these genes. As seen in Figure 1C, all of the new family members were found to be transcribed. *CLE41* was the most abundantly expressed gene of the five in all organs examined. No amplification was observed from mock reactions that lacked reverse transcriptase (data not shown). The bioinformatic and molecular data together suggest that *CLE41* to *45* are genuine, transcribed members of the *CLE* family.

CLE Gene Transgenic Arabidopsis Plants Overexpressed the Transgene and Displayed Strong Penetrance of Phenotype

Seventeen of the 31 Arabidopsis *CLE* genes representing the three major phylogenetic clades (Fig. 1B), other family members, as well as *CLV3* were cloned downstream of the cauliflower mosaic virus 35S promoter and transformed into Arabidopsis (Table I). A maximum of 24 individual kanamycin-resistant T_1 plants from a transformation cohort were used for further phenotypic analysis. In cases where fewer than 24 transformants were available, no fewer than 12 plants were examined. Plants from independent floral-dip experiments revealed no differences in phenotype with a given transgene (data not shown).

Although there was variability in the severity of the phenotypes, we observed that, within a cohort, 90% to 100% of the plants displayed similar phenotypes in all 18 lines examined. To determine that the observed phenotypes were due to overexpression of the gene, rather than gene silencing, we performed RNA-blot analysis on plants displaying a range of phenotypic strengths from each line. We observed that the transgenes were expressed in most of the plants that we examined, but a few plants did not display detectable levels of the transgene (Fig. 3). However, we were never able to detect expression of any of the endogenous *CLE* genes or *CLV3* on the blots (Fig. 3). Furthermore, these plants displayed phenotypes consistent with those of plants with detectable transgene expression, so our inability to detect expression of the *CLE* transgenes in these plants cannot be interpreted as evidence of gene silencing.

Overexpression of the *CLE* Genes Results in Developmental Timing Delays

We conducted a detailed examination of the phenotypes of the *CLE* gene-overexpressing lines based on the developmental staging scheme of Boyes et al. (2001). Key developmental stages were logged as were morphological abnormalities. Developmental timing delays were observed consistently in all of the *CLE* transgene cohorts relative to empty-vector controls (Fig. 4A). The average time to the first floral bud (stage 5.10; Boyes et al., 2001) in empty-vector control plants was approximately 16 d after germination (DAG) under the

Figure 2. (*Continued.*)
long roots, and low mortality of the transformed plants prior to developmental stage 5.10. Aii, CLE domain sequences of the *wus*-like CLE genes that showed dwarfing at 14 and 21 DAG, short roots, and had >50% mortality of the transformed plants prior to flowering. B, Dwarf phenotype. C, Shrub-like phenotype. D, Long-root phenotype. Predicted phenotypic classes for *CLE* genes in a 35S promoter overexpression experiment appear to the right of the CLE domain sequences for which there are presently no data. Amino acid residues in these conceptual sequences that are found in 20 or more CLE domain sequences are highlighted in light gray. Amino acid residues that differ from the consensus sequence found in 20 or more CLE domain sequences are highlighted in dark gray. Amino acid residues that differ from the main consensus and that correlate with a specific phenotypic class are highlighted in black. The major phylogenetic clades are highlighted with red, blue, and green backgrounds as in Figure 1.

Table I. *Summary of phenotypes resulting from CLE gene family member overexpression*

Gene (Background)[a]	Phenotype							
	wus-Like	Developmental Timing Delays[b]	Anthocyanin	Root Length[b]	Dwarf (14 DAG)[b]	Dwarf (21 DAG)[b]	>50% Mortality (Stage 5.10)[c]	Apical Dominance
CLV3	Y	Y	Y	Short	ND[d]	ND	67%	N
CLE2	Y	Y	N	Long	N	Y	N	N
CLE3	Y	Y	N	NC[e]	N	Y	N	N
CLE4	Y	Y	N	Long	ND	Y	N	N
CLE4 (Ler; clv3-2)	Y	Y	N	ND	N	Y	N	N
CLE5	Y	Y	N	Long	N	Y	N	N
CLE6	Y	Y	N	Long	N	Y	N	N
CLE7	Y	Y	N	Long	N	Y	N	N
CLE9	Y	Y	Y	Short	Y	Y	67%	N
CLE10	Y	Y	Y	Short	Y	Y	92%	N
CLE11	Y	Y	N	Short	Y	Y	92%	N
CLE13	Y	Y	Y	Short	Y	Y	96%	N
CLE18	N	Y	N	Long	N	N	N	Y
CLE19	N	Y	Y	Short	Y	Y	N	Y
CLE21	N	Y	Y	Short	Y	Y	N	Y
CLE25	N	Y	N	Long	N	N	N	Y
CLE26	N	Y	N	Long	N	N	N	Y
CLE42	N	Y	N	NC	Y	Y	N	N
CLE44	N	Y	N	NC	Y	Y	N	N

[a]Genetic background was Col-0 unless otherwise specified. [b]Relative to empty-vector control. [c]Only lines that showed >50% mortality prior to the appearance of the first floral bud (stage 5.10) are specified. [d]ND, Not done. [e]NC, No change.

long-day conditions used in these experiments. The time taken to reach stage 5.10 in the *CLE*-overexpressing cohorts ranged between 23 and 56 DAG (Fig. 4A) as compared to 16 and 59 d for empty-vector negative controls and *CLV3* positive controls. The *CLE11*- and *CLE13*-overexpressing plants reached stage 5.10 at 56 DAG, but only one plant from each cohort survived to flower (Fig. 4A). Once a floral bud was observed, the time to the appearance of an open flower (stage 6.00) was far less variable than the time to stage 5.10, ranging between 0 and 8 d, compared with 4 d for empty-vector controls. *CLE10*, *11*, and *13* (0 d) and *CLV3*, *CLE16*, and *CLE25* (8 d) were at the extremes of this range. The observation of 0 d between observation of the first flower and observation of the first open flower merely reflects that by the time the first flower was observed it was already open.

To examine possible differences in overexpression phenotypes among *wus*-like *CLE* gene family members more closely, we conducted a more detailed developmental stage-based phenotypic examination of plants overexpressing *CLE4* and *CLV3* as representatives of the two classes of *wus*-like phenotype overexpressers (OEs). Developmental timing delays in the *CLE4*OE and *CLV3*OE plants relative to empty-vector controls for multiple developmental stages were observed (Fig. 5A). At all developmental stages, the *CLV3*OE lines were more severely delayed than the *CLE4*OE lines. The relative strength of the *CLV3*OE phenotype as compared with empty-vector controls and *CLE4*OE lines was again observed in the development and elongation of the inflorescence (Fig. 5B). In addition to the greater delay in the onset of flowering (Fig. 5B), *CLV3*OE plants manifested decreased inflorescence elongation rates relative to the *CLE4*OE plants, as well as a more severely decreased terminal height of the inflorescence relative to empty-vector controls (Fig. 5B). Furthermore, the growth curve of the inflorescences in

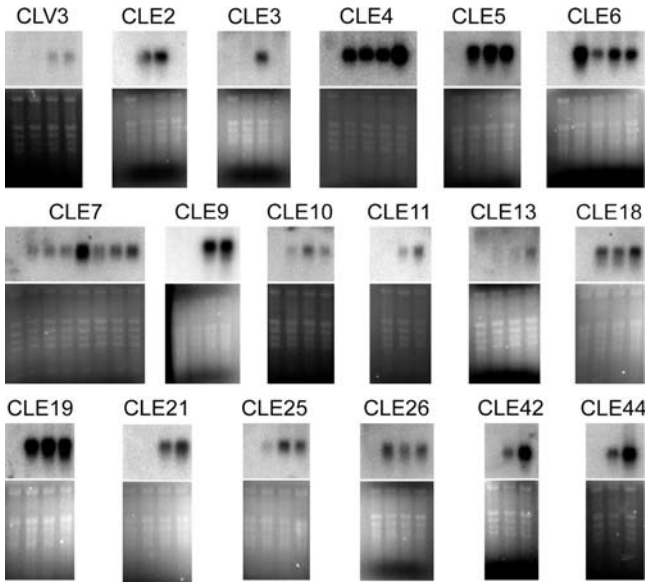

Figure 3. RNA-blot hybridization analysis of plants harboring *CLE* gene overexpression constructs. The leftmost lanes of all blots are negative control RNA from plants transformed with empty-vector constructs. Between two and seven kanamycin-resistant plants displaying varying phenotypic severity were used in RNA blots. Probes corresponded to the genes with which the plants were transformed. RNA loading controls are shown beneath the hybridization autoradiograms.

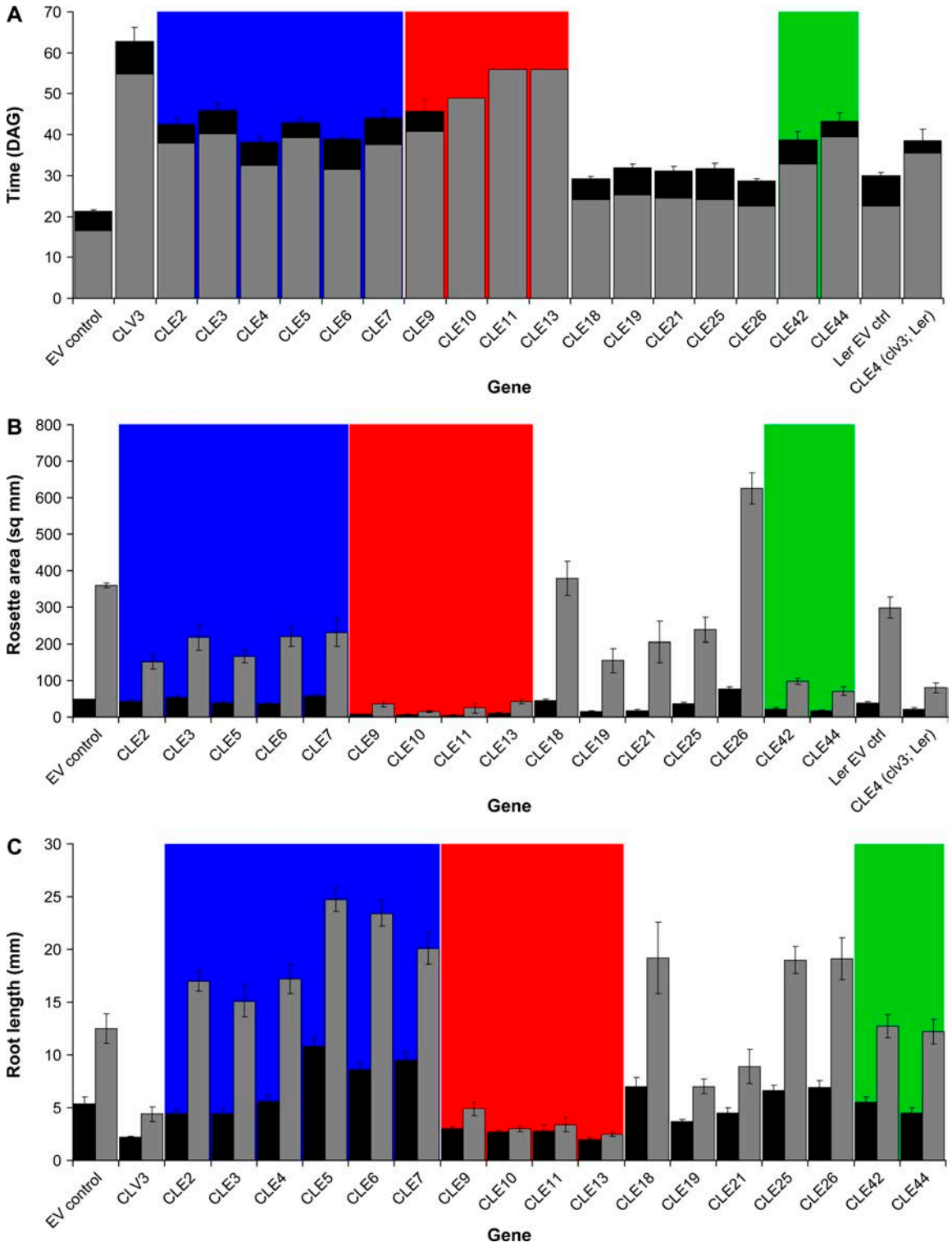

Figure 4. Developmental timing, rosette areas and root lengths of plants overexpressing *CLV3*, and various *CLE* genes. All plants were of the Col-0 genetic background unless otherwise specified. A, Times to stage 5.10 (gray portions of bars) and 6.00 (black portions of bars; Boyes et al., 2001) are shown. Transgene overexpressers are compared to EV control and *CLV3*OE positive control. CLE4 (clv3; L*er*) signifies the overexpression of the 35S-CLE4 gene in a *clv3-2* mutant in the L*er* genetic background. Error bars represent the SE. B, Rosette areas were derived from image analysis data acquired 14 (black bars) and 21 DAG (gray bars). Transgene overexpressers are compared to EV control. CLE4 (clv3; L*er*) signifies the overexpression of the 35S-*CLE4* gene in a *clv3-2* mutant in the L*er* genetic background. The other plants in the figure are of the Col-0 ecotype. Error bars represent the SE. C, Root lengths were measured 8 DAG (black bars) and 11 DAG (gray bars). Transgene overexpressers are compared to EV control and *CLV3*OE positive control. The major phylogenetic clades are highlighted with blue, red, and green backgrounds as in Figure 1B. EV control, Empty-vector control.

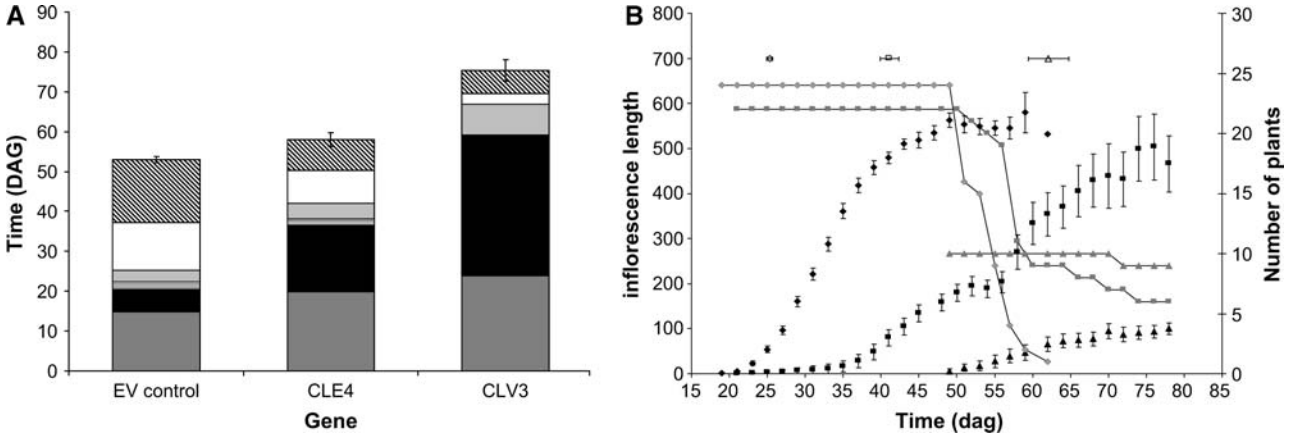

Figure 5. Relative effects of *CLE4* and *CLV3* overexpression as compared to EV controls. A, Developmental stage timing of EV control, CLE4-, and CLV3-overexpressing plants. Dark gray, Stage 1.08 (eight leaves); black, stage 5.10 (first floral bud); horizontal stripes, measurable inflorescence stem; light gray, stage 6.00 (first open flower); white, stage 6.50 (flowering 50% complete); diagonal stripes, stage 6.90 (flowering complete). Error bars represent the SE. B, Average flowering time is represented by the white symbols at the top of the figure. Mean inflorescence lengths are represented by the black symbols, with the scale on the left side of the graph. Plant counts are represented by the gray symbols, with the scale on the right side of the graph. EV control plants are represented by diamonds, *CLV3*OE plants are represented by triangles, and *CLE4*OE plants are represented by squares. Error bars represent the SE. EV control, Empty-vector control.

the *CLE4*OE and *CLV3*OE cohorts displayed less of a sigmoidal shape than was observed for empty-vector controls (Fig. 5B).

Overexpression of Many *CLE* Genes Results in Phenotypes Similar to CLV3 Overexpression

Overexpression of *CLE* genes *2*, *3*, *4*, *5*, *6*, *7*, *9*, *10*, *11*, and *13* all resulted in pleiotropic phenotypes similar to the phenotypes described for the overexpression of *CLV3*, *CLE40*, and the plant parasitic nematode gene *Hg-SYV46* (Brand et al., 2000; Hobe et al., 2003; Wang et al., 2005). This phenotype was initially characterized by arrest of new leaf development from the SAM (Fig. 6, B–D). Often, the plants recovered from the loss of the SAM by the release of axillary buds. Growth from the axillary buds eventually terminated and secondary axillary buds were released, and so on, a phenotype very similar to *wus* loss-of-function mutants (Laux et al., 1996). Therefore, we denote such plants as displaying a *wus*-like phenotype (Fig. 2A, category A). The cumulative effects of overexpression of these genes were large plants with multiple shoots and thick, fleshy, misshapen leaves (Fig. 6, E–G). This phenotype was the most pronounced in *CLV3*-overexpressing positive control plants. The plants that overexpressed *CLE2*, *3*, *4*, *5*, *6*, and *7* (the Aii subcategory among the *wus*-like phenotype plants; Fig. 2A) had milder phenotypes than those that overexpressed *CLE9*, *10*, *11*, and *13* (the Ai subcategory among the *wus*-like phenotype plants; Fig. 2A), with low mortality prior to flowering. Leaves, while still misshapen in *wus*-like Aii plants, were not as distorted as those in the Ai subcategory (Figs. 2A and 6, E–G).

Similar to published observations in which only 16% of plants that overexpressed *CLV3* resumed growth after the initial SAM arrest (Brand et al., 2000), a large fraction of plants overexpressing *CLV3*, *CLE9*, *CLE10*, *CLE11*, and *CLE13* never recovered from the initial developmental arrest. Between 67% and 96% of these plants died before they flowered (the Ai subcategory among the *wus*-like phenotype plants [Fig. 2A; Table I]). We found that 67% of the *CLV3*OE plants never resumed growth after the initial SAM arrest (Table I).

Other developmental abnormalities were noted in the *wus*-like plants. In addition to misshapen leaves, plants occasionally displayed bell- or cup-shaped leaves (Fig. 6, H and R). Floral phenotypes consistent with those previously described for *CLV3*OEs (Brand et al., 2000; Hobe et al., 2003) were observed in the *wus*-like plants. Flowers often lacked carpels and had fewer anthers than normal or completely lacked anthers (Fig. 6, J–L). No effect on the outer whorl petal and sepal numbers was observed. All the plants displaying the *wus*-like phenotype had smaller rosette areas than empty-vector controls at 21 DAG (Fig. 4B). However, only plants that overexpressed *CLE9*, *10*, *11*, and *13* (category Ai) had smaller rosette areas compared to controls at 14 DAG (Fig. 4B). A further difference between the *wus*-like Ai and Aii phenotypes was observed in the seedling primary root length measurements. Like the CLV3 positive control plants, Ai category plants displayed severe inhibition of root elongation, whereas Aii category plants displayed varying degrees of stimulation of root elongation relative to empty-vector controls (Fig. 4C). These observations correlate precisely with the differences observed in rosette area in that all lines that displayed dwarfing at 14 and 21 DAG and high mortality also displayed severe inhibition of root elongation (Fig. 4, B and C; Table I).

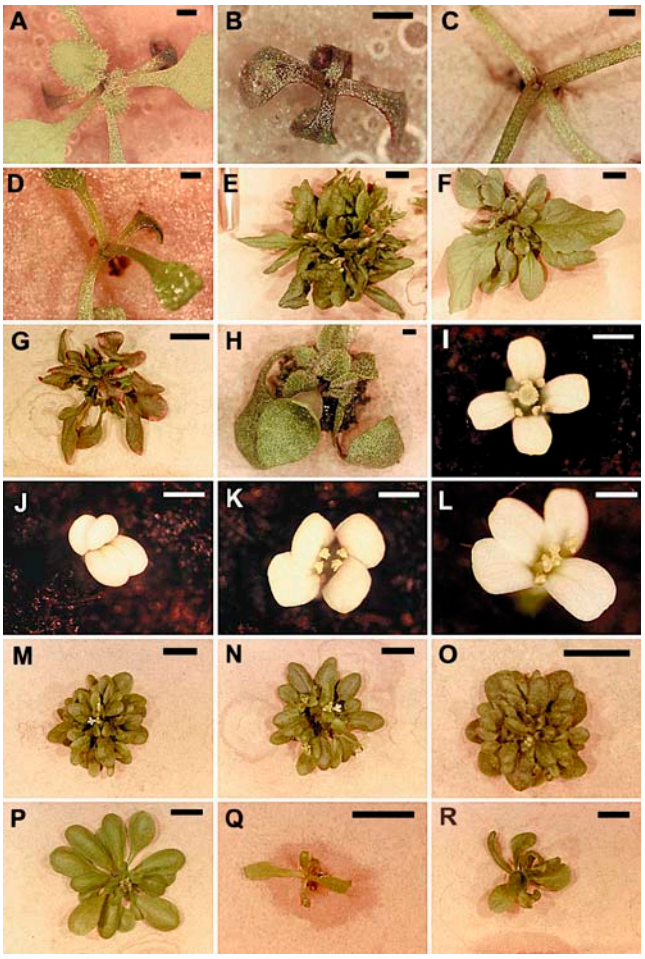

Figure 6. Overexpression phenotypes of *CLE* family members. A, Empty-vector control plant, 14 DAG. B, *CLV3*-overexpressing control plant, 14 DAG, showing SAM arrest and anthocyanin overproduction. C, *CLE2*-overexpressing plant, 14 DAG, showing SAM arrest. D, *CLE4*-overexpressing plant, 14 DAG, showing SAM arrest. E, *CLV3*-overexpressing plant, stage 5.10 (appearance of first floral bud), showing misshapen leaves and irregular phyllotaxis. F, *CLE4*-overexpressing plant, stage 5.10, showing misshapen leaves and irregular phyllotaxis. G, *CLE10*-overexpressing plant, 56 DAG, showing misshapen leaves, irregular phyllotaxis, and anthocyanin overproduction. H, *CLE2*-overexpressing plant, 56 DAG, terminating in a bell-shaped leaf. I, Empty-vector control flower. J, *CLV3*-overexpressing flower, showing a lack of carpels and stamens. K, *CLE4*-overexpressing flower, lacking carpels and two stamens. L, *CLE2*-overexpressing flower, lacking carpels and one stamen. M, *CLE42*-overexpressing plant, 63 DAG, displaying weak shrub-like phenotype. N, *CLE44*-overexpressing plant, 63 DAG, displaying weak shrub-like phenotype. O, *CLE44*-overexpressing plant, 63 DAG, displaying an intermediate shrub-like phenotype. P, *clv3-2* mutant plant, stage 6.00 (first open flower). Q, *clv3-2 CLE4*-overexpressing plant, 7 DAG, showing SAM arrest. R, *clv3-2 CLE4*-overexpressing plant, 28 DAG, displaying a bell-shaped leaf. Cauliflower mosaic virus 35S promoter was used for all gene overexpression. Scale bars: A to D and H to L = 1 mm; E to G and M to R = 1 cm.

Overexpression of Some CLE Genes Results in Dwarf Plants But Not Termination of the SAM

The second major class of phenotype we observed was one of dwarfing and developmental timing delays, but no apparent termination of the SAM (Fig. 4, A and B), denoted here as the dwarf phenotype or category B (Table I; Figs. 1B and 2B). Plants that overexpressed *CLE 19*, *21*, and *25* were all observed to be in this category. *CLE19*OEs and *CLE21*OEs displayed dark green/purplish leaves, suggesting anthocyanin overproduction in these plants (Fig. 2). Leaf size was smaller in these cohorts relative to empty-vector controls, and some leaf curling was observed (data not shown). However, the leaves in these cohorts were never observed to have a misshapen character. Furthermore, the *CLE19*, *21*, and *25* overexpression cohorts consistently displayed development of new leaves from the shoot apex. Root elongation of the plants in the dwarf category was either mildly inhibited relative to empty-vector controls in *CLE19*OEs and *CLE21*OEs or even stimulated in *CLE25*OEs (Fig. 4C).

The *CLE42* and *CLE44* overexpression cohorts were also composed of dwarf plants that exhibited developmental timing delays (Fig. 4, A and B). Unlike the members of the dwarf phenotype class, these cohorts displayed rosettes that apparently lacked apical dominance, with small, rounded leaves, resulting in a compact, shrub-like phenotype (Figs. 1B, 2C, and 6, M–O). The phenotypes of the *CLE42* and *CLE44* overexpression cohorts were virtually identical. The shrub-like phenotype observed in these cohorts was vaguely reminiscent of the *wus*-like phenotype observed in many *CLE* gene-overexpressing plants (Table I; compare Fig. 6, E–H with Fig. 6, M–O). However, we never observed misshapen leaves or arrest of growth from the SAM. Furthermore, these plants were dwarves throughout their lives (Fig. 4B; data not shown). Flowering was delayed (Fig. 4A), but floral development and fertility were unaffected in these plants (data not shown). Root elongation was also unaffected by the overexpression of these genes (Fig. 4C).

Two *CLE* overexpression cohorts, *CLE18* and *CLE26*, could not be categorized into the *wus*-like, dwarf, or shrub-like phenotypic classes. No obvious morphological phenotypes were observed in rosettes of plants that overexpressed these genes. However, root elongation in these lines was greater than that of empty-vector controls both 8 and 11 DAG (Fig. 4C). Furthermore, the mean rosette area of *CLE26*-overexpressing plants was greater than that of controls at 14 and 21 DAG (Fig. 4B). This phenotype is denoted as the long-root phenotype (Figs. 1B and 2D).

CLE4 Overexpression Overrides the *clv3* Mutant Phenotype

Although overexpression of many of the *CLE* genes results in phenotypes very similar to that of *CLV3* gene overexpression, suggesting that the CLE proteins are transmitting a signal through the CLV1/2 receptor complex, it is possible that the phenotypes they are generating are in fact through an interaction with a receptor other than CLV1/2. To test these hypotheses, we transformed both *clv1-1* and *clv3-2* plants with the

CLE4 gene. We found that *CLE4* overexpression did not complement the *clv1-1* mutation (data not shown), but strong expressers of *CLE4* were able to completely override the *clv3-2* mutant phenotype, resulting in plants that displayed a *wus*-like phenotype (Fig. 6, P–R). We observed cessation of growth from the SAMs of these plants at the seedling stage (Fig. 6Q) and from axillary meristems (data not shown). Like other cohorts that displayed the *wus*-like phenotype, we occasionally observed bell-shaped terminal leaves in the *clv3-2 CLE4*-overexpressing cohort (Fig. 6R). The *CLE4*-overexpressing *clv3* mutant plants displayed developmental timing delays (Fig. 4A) and dwarf rosettes relative to Landsberg *erecta* (L*er*) empty-vector controls (Fig. 4B).

DISCUSSION

Many *CLE* Genes Exhibit the Potential for Functional Redundancy with *CLV3*

The overexpression of 10 of the Arabidopsis *CLE* genes that we tested resulted in phenotypes similar to that of overexpression of *CLV3* itself (Table I; Figs. 2A and 4–6). The simplest interpretation of these results is that the functions of proteins encoded by these genes are redundant with those of CLV3. Such mimicry of the *CLV3* overexpression phenotype has also been observed with *CLE40* and *Hg-SYV46*. The ability of CLE40 to functionally substitute for CLV3 was elegantly demonstrated by expressing the *CLE40* gene under the control of the *CLV3* promoter (Hobe et al., 2003). However, it was further shown that a *cle40* mutation did not affect shoot growth, but rather resulted in defects in root growth and development (Hobe et al., 2003). In the case of the plant parasitic nematode *Hg-SYV46* gene, it appears that the protein product encoded by this gene is secreted by the parasites, possibly to alter root cell development to facilitate feeding (Olsen and Skriver, 2003; Wang et al., 2005). In light of these findings, any hypothesis regarding natural functional redundancy of *CLE* genes capable of causing the *wus*-like overexpression phenotype must be tested carefully. The ability of overexpressed *CLE4* to override the *clv*3 mutation and bring about the *wus*-like phenotype demonstrates that the CLE4 protein is also capable of acting in a functionally redundant manner to CLV3 and that CLE4 action is independent of CLV3. Based on our data, it seems likely that if *CLE4* were expressed under the control of the *CLV3* promoter, complementation of *clv*3 would also result. By inference, our results and those of Hobe et al. (2003) suggest that all of the *CLE* genes that confer the *wus*-like phenotype would be capable of complementing *clv3* mutants when expressed under the control of the *CLV3* promoter. The root-predominant expression of *CLE4*, coupled with a lack of expression in shoot apices (Sharma et al., 2003b), suggests that its protein product, like CLE40 (Hobe et al., 2003), does not naturally play a role in SAM maintenance. Nonetheless, our results do not conclusively rule out that CLE4 or one of the other CLE proteins may in fact interact with the CLV1/2 complex. If this is the case, CLE9, 10, 11, and 13 appear to be the most likely candidates to play such a role, based on their gene overexpression phenotypes (Table I) and expression profiles (Sharma et al., 2003b).

Overexpression of *CLE4* in the *clv1-1* mutant background failed to complement or otherwise alter the mutant phenotype (data not shown). However, the recent demonstration that *clv1-1* and other strong-to-intermediate phenotype *clv1* alleles are dominant negative makes this result difficult to interpret, as the dominant-negative phenotype appears to mask the activity of functionally redundant receptors in Arabidopsis that also play roles in the regulation of SAM size (Diévart et al., 2003).

Other Phenotypes Suggest Diversity of Function for *CLE* Gene Family Members

Among the *CLE* genes whose overexpression did not confer a *wus*-like phenotype, two classes of dwarf phenotypes were observed. Miniature rosettes and inflorescences, often accompanied by high mortality, apparent anthocyanin overproduction, and developmental timing delays characterize the dwarf phenotype, as found in plants that overexpressed *CLE19*, *21*, and *25* (Table I; Figs. 2 and 4). The overexpression phenotypes of these plants suggest possible roles for these *CLE* family members in the regulation of plant stature and stress responses.

Abundant small leaves and bushy rosettes brought about by a lack of apical dominance and strongly delayed flowering characterize the shrub-like phenotype exemplified by the new *CLE* family members *CLE42* and *CLE44* (Table I; Figs. 2, 4, 5, and 6, M–O). Neither misshapen leaves, high mortality rates, nor anthocyanin overproduction are observed in these plants. The overexpression phenotypes of these plants suggest that CLE42 and CLE44 may have potentially redundant roles in regulating apical dominance and organ size. Recent work suggests that the Leu-rich repeat-receptor-like kinase receptor ERECTA plays a role in regulating organ shape and possibly apical dominance. It has also been demonstrated that there are functionally overlapping receptors to ERECTA (Shpak et al., 2004). It will be interesting to examine the *CLE42* and *CLE44* overexpression phenotypes in an *erecta* null mutant as well as in *clv1* and *clv2* null mutants to more accurately determine the relationship of these ligands to these important developmental receptors.

Relationship of Overexpression Phenotypes to Phylogeny and Sequences in the CLE Domains

Alignments of predicted CLE protein sequences show that there is very little conservation of amino

acid sequence in the *CLE* gene family, with the exception of the CLE domain itself (Cock and McCormick, 2001). Therefore, the similarities of the observed overexpression phenotypes correlating with phylogenetic clades of the *CLE* genes (compare Fig. 4 with Fig. 1B) are likely to be largely, if not entirely, attributable to the CLE domains. We therefore examined the CLE domains of the predicted proteins in light of the overexpression phenotypes conferred by the genes (Fig. 2). Two distinct phenotypic subclasses were observed in plants that displayed the *wus*-like phenotypes. Specifically, although *CLE2*, *3*, *4*, *5*, *6*, *7*, *9*, *10*, *11*, and *13* all displayed the *wus*-like phenotype, *CLE 9*, *10*, *11*, and *13*OEs displayed stronger dwarf phenotypes, shorter roots, and higher mortality rates than did *CLE2*, *3*, *4*, *5*, *6*, and *7*OEs (Figs. 2 and 4; Table I). We found differences in the CLE domains of these predicted proteins that correlated perfectly with our phenotypic data (Fig. 2). The conceptual CLV3, CLE40, and CLE9, 10, 11, and 13 proteins all closely matched the CLE domain consensus. All these predicted proteins, except CLE40, matched the CLE domain consensus at the eight best conserved residues in the CLE domain, specifically the Arg, Val, Pro, Gly, Pro, Pro, Leu, and His residues at positions 3, 5, 6, 8, 9, 11, 12, and 13, respectively (numbering as in Fig. 2, shaded in light gray when conserved), conforming to the consensus EKRLVPSGPNPL(H/N). In contrast to the CLE9, 10, 11, and 13 high-mortality, strong dwarf *wus*-like phenotypes (Ai subcategory), the CLE domains of the overexpressed genes that conferred the low-mortality, weak dwarf *wus*-like phenotypes (Aii subcategory) had distinct CLE domain sequences that perfectly correlated with the observed overexpression phenotypes and phylogenetic classification (Fig. 2). Specifically, the CLE2, 3, 4, 5, 6, and 7 CLE domains differed from the conserved Val at position 5 with a Ser, a Gly at position 7, rather than the conserved Ser and a Gln (CLE2, 5, 6, and 7) or Arg (CLE3 and CLE4) at position 12 in place of the conserved Leu (these three residues are shaded in black in Fig. 2 when present). Remarkably, these three changes from the Ai subcategory consensus were always found in tandem, and plants that overexpressed genes with this consensus [S (charged residue) RLSPGGPDPQHH] always conferred the low-mortality, weak dwarf *wus*-like phenotype. Therefore, the simplest interpretation of our results is that the CLE domain differences at positions 5, 7, and 12 are likely responsible for the differences in observed *wus*-like subcategories (Figs. 1B and 2A). Our data cannot distinguish whether these phenotypic differences are due to differences in strength of signal transmitted through the CLV1/2 complex upon overexpression or to interaction with another, as yet unknown, receptor.

Insufficient data exist for definitive inclusion of *CLV3* or *CLE4* in group Ai or Aii. This is because the phenotypic analysis for these two genes was performed under a different regime than for the other CLE genes, as described. Therefore, we do not have data on rosette areas at 14 and 21 DAG. However, *CLV3*OEs exhibit high mortality (Table I) and inhibition of root elongation (Fig. 4C) and most *CLE40*OEs fail to develop past the germination stage (Hobe et al., 2003), which we equate with the high-mortality phenotype. Therefore, these genes likely belong in *wus*-like category Ai. In contrast, *CLE4*OEs exhibit low mortality (Table I) and an apparent stimulation of root elongation (Fig. 4C), which suggests that *CLE4* belongs in *wus*-like category Aii.

The CLE1 and CLE12 CLE domain sequences conform to subcategories Aii and Ai, respectively, but we have no experimental data to allow their definitive categorization (Fig. 2). Based on our findings, we predict that the *CLE1* overexpression phenotype will conform to the Aii subcategory and that the *CLE12* overexpression phenotype will conform to an Ai subcategory when overexpressed under the control of the 35S promoter under the same conditions that we used in this study.

Similar to the *wus*-like phenotypes, there is a distinct correlation of the phenotypes of *CLE42* and *CLE44* overexpression cohorts and their predicted CLE domain amino acid sequences. Plants that overexpressed these newly discovered genes displayed a shrub-like rosette phenotype, with small, rounded leaves and a lack of apical dominance (Fig. 6, M–O). This phenotype is correlated in both cases with the substitution of a His residue for the otherwise absolutely conserved Arg at position 3 in the main CLE domain consensus, an Ile residue at position 12, and a Ser at the otherwise absolutely conserved His at position 13 (Fig. 2C), resulting in the category C consensus XXHGVPSGPNPISN (Fig. 2C). The His and Ser substitutions always occur in tandem and are also always correlated with the Ile substitution at position 12 (highlighted in black in Fig. 2C). However, several other CLE domains possess an Ile residue at position 12 (Fig. 2). We note that the predicted CLE41 protein is virtually identical to the predicted CLE44 in the CLE domain (Fig. 2). In fact, CLE41, 42, and 44 are the only three predicted proteins to diverge from the main consensus at positions 3 and 13. We therefore predict that overexpression of *CLE41* would result in the shrub-like rosette (category C) phenotype in Arabidopsis plants.

There is no strong consensus in the CLE domain among the genes whose overexpression resulted in the dwarf (category B; Fig. 2B) or long-root phenotypes (category D; Fig. 2D), with the consensus sequences SKRXIPSGPDPLHN and X(charged residue) RXXPXGPDPXHN, respectively. In fact, the category B consensus is a subset of the category D consensus. It is possible that the dwarf phenotypes are not evidence of functional redundancy to one another, but rather neomorphic effects of the overexpression of genes that play distinct developmental roles. Additionally, we cannot rule out the requirement for other portions of the CLE proteins for the conferral of any of these phenotypes. However, recent findings that exogenous application of CLV3, CLE19, and CLE40 CLE domain

synthetic peptides to Arabidopsis roots causes root apical meristem consumption (Fiers et al., 2005) demonstrates that the CLE domain alone is sufficient for this phenotype at least. In any case, these phenotypes, together with the shrub-like phenotypes and the differences in the two subcategories of the *wus*-like phenotypes, suggest the interaction with a receptor or receptors other than the CLV1/2 complex. Among the remaining untested genes, *CLE8*, *14*, *16*, *17*, *20*, *22*, *27*, *43*, and *45*, we do not consider that we have sufficient data to predict their overexpression phenotypes because these all harbor substitutions making them inconsistent with the main phenotypic classes.

Pleiotropy of the *CLE* Gene Overexpression Phenotypes Suggests Ectopic Interactions with Multiple Receptors

Virtually all of the *CLE* gene overexpression phenotypes are pleiotropic. For example, in *CLV3* and many *CLE*-overexpressing plants, not only was maintenance of the SAM disrupted (Fig. 6, B–E), but also root development was stunted (Fig. 4C), leaves were highly variable in size and misshapen (Fig. 6, E–H), inflorescence elongation was inhibited (Fig. 6B), developmental timing was delayed (Fig. 4A), and plants displayed varying degrees of dwarfism (Fig. 4B). Many of these phenotypes can be explained simply by SAM arrest. However, the effects of *CLV3* and *CLE4* overexpression on root elongation and the distorted leaf morphologies of *CLE* genes that conferred the *wus*-like phenotypes are difficult to explain in such reductionist terms. In our experiments, the overexpression of *CLE 2* to *7*, *9*, *10*, *11*, and *13* all resulted in *wus*-like phenotypes, implying that their overexpression phenotypes were due in part to interaction with the CLV1/2 receptor complex, similar to *CLV3* overexpression. However, only *CLE2* to *7* overexpression appeared to cause the less severe phenotypes, with milder effects on early dwarfing, low mortality, and stimulation of root elongation. The fact that the overexpression phenotypes of these genes and the other *CLE* genes were not all identical to and, in many cases, dramatically different from that of *CLV3* implies that these genes are exerting effects through their native receptors and perhaps other non-native receptors in addition to the CLV1/2 complex. A prediction of this hypothesis is that phenotypic effects of the overexpression of the *CLE* genes not due to SAM arrest effects in aboveground portions of plants should be observable in *clv1* null mutants such as *clv1-6* and *clv1-7*, rather than dominant-negative mutants such as *clv1-1* and *clv1-4* (Diévart et al., 2003). In such experiments, phenotypes resulting from interaction with the putative native receptor for a given *CLE* gene should be separable from effects resulting from ectopic interaction with the CLV1/2 receptor complex. Conversely, the effects of interaction of CLV3 with a non-native receptor or receptors in *clv1* or *clv2* mutant backgrounds should be helpful in determining which overexpression phenotypes observed in wild-type genetic backgrounds are due to interaction with non-native receptors, if any. The finding of Fiers et al. (2005) that exogenous application of CLV3 peptide to roots of *clv1-1* plants causes root stunting supports this hypothesis. However, further insight into CLV3 interaction with non-native receptors in aboveground portions of the plant will likely require the use of true null mutants, as discussed above.

CONCLUSION

A growing body of evidence suggests that the *CLE* genes constitute an ancient, functionally conserved gene family that plays important roles in plant growth and development. The systems approach we have taken to the phenotypic analysis of the *CLE* gene family has yielded a wealth of data on the effects of overexpression of these genes. This information has allowed us to formulate testable hypotheses as to possible functional roles of these genes. The *CLE* gene overexpression phenotypes have also allowed us to hypothesize that amino acid residue changes at specific positions within the predicted CLE protein sequences may be responsible for the different phenotypes conferred by overexpression of these genes. These amino acids may be responsible for conferring different specificities to homologous receptors. Some of these receptors may be involved in functionally overlapping signaling processes as has been shown for the ERL receptors (Shpak et al., 2004), whereas others could be involved in diverse developmental processes, based on our observations. Based on the CLV3 paradigm (Bäurle and Laux, 2003; Carles and Fletcher, 2003; Doerner, 2003; Sharma et al., 2003a), the 31 Arabidopsis CLE ligands are likely to interact with members of the Leu-rich repeat-receptor-like kinase receptor family, of which there are more than 400 members (Shiu and Bleecker, 2001). The identification of all the cognate receptors for the CLE proteins will therefore likely be a formidable task. Our findings may simplify this task because the phenotypic similarities resulting from the overexpression of many of these genes suggest that such receptors are likely those molecules most closely related to CLV1 and CLV2.

MATERIALS AND METHODS

Bioinformatic Analysis

The Arabidopsis (*Arabidopsis thaliana*) genome sequence (Arabidopsis Genome Initiative, 2000) was scanned for putative *CLE* family members via a TBLASTN search (Altschul et al., 1997) with CLV3 as the query sequence. Examination of initial candidate TBLASTN hits revealed that the *CLE* gene family members lacked introns. Subsequent candidate TBLASTN hits were then examined for open reading frames with putative signal peptide sequences approximately 100 bp upstream of the conserved region. DNA sequences meeting these criteria were conceptually translated and aligned using ClustalX 1.81 software (Thompson et al., 1997). Bootstrap neighbor-joining analysis (1,000 iterations) was performed using PAUP* 4.0b10 (Sinauer Associates). A graphic representation of the bootstrap analysis data was generated using TreeView 1.6.6 (Page, 1996).

Plant DNA Preparation and Transgene Construction

Arabidopsis L. Heynh. cv Col-0 genomic DNA was prepared from leaves via TRIzol (Invitrogen) extraction. Primers were designed with Gateway (Invitrogen)-compatible 5′ ends. The *CLE* family genes were amplified via 30 cycles of PCR using Advantage 2 polymerase (BD Biosciences-CLONTECH). PCR products were cloned into pDonorAMP (Invitrogen) using the Gateway BP reaction and transformed into *Escherichia coli* strain DH5α. Inserts were transferred via the Gateway LR reaction into pART27 (Gleave, 1992) modified to contain the pART7 T-DNA (Gleave, 1992) with Gateway LR sites in the polylinker. LR reaction products were transformed into DH5α and positive transformants were sequence verified and electroporated into *Agrobacterium tumefaciens* strain LBA4404.

RNA Preparation, RNA-Blot Analysis, Complementary DNA Synthesis, Primer Design, and Real-Time PCR Analysis of Gene Expression

Arabidopsis total RNA was prepared from various organs via TRIzol (Invitrogen) extraction. RNA blots were performed as described (Sambrook et al., 1989) onto Hybond N+ membranes (Amersham Biosciences). ^{32}P-labeled DNA probes were made using α-[^{32}P]dCTP with Rediprime II kits and purified on ProbeQuant G-50 microcolumns, using instructions provided by the manufacturer (Amersham Biosciences). Probes were denatured by boiling and snap cooling and hybridizations were carried out overnight in Ultrahyb hybridization buffer (Ambion) with instructions as provided by the manufacturer. Blots were visualized utilizing a Typhoon phosphor imager (Amersham Biosciences). For real-time PCR analysis, first-strand cDNA was synthesized from RNA templates using SuperScript III reverse transcriptase (Invitrogen) with instructions as provided by the manufacturer. Primers optimized for real-time PCR analysis were designed using PrimerExpress 2.0 software (Applied Biosystems). Real-time quantitation of cDNA expression levels was conducted using an ABI 9600 cycler and SYBR Green master mix (Applied Biosystems) for fluorescent detection of products. Analysis of data was facilitated by the use of the sequence detection system (Applied Biosystems) software.

Plant Material

Arabidopsis ecotype Col-0 plants were used for transgenic experiments. The *clv* mutant lines were obtained from the Nottingham Arabidopsis Stock Centre (NASC). Transgenic plants were created via the floral-dip method (Clough and Bent, 1998). T1 generation seeds were surface sterilized and transformed seedlings were selected on 0.5× Murashige and Skoog medium containing 50 μg/mL kanamycin sulfate and 100 μg/mL timentin. Transformed plants were transferred to rockwool substrate (Grodan) and grown at 22°C and 60% humidity under 150 μmol m^{-2} s^{-1} of white light with a 16-h daylength, using hydroponic nutrient medium at pH 5.7 (Gibeaut et al., 1997), buffered with 0.5 mM MES.

Plant Phenotypic Analysis

Phenotypic examination was based on the developmental staging scheme of Boyes et al. (2001). Two examination schemes were used. For *CLV3*- and *CLE4*-overexpressing plants, seeds were stratified at 4°C for 3 d. Primary root lengths of experimental and same-day empty-vector control seedlings were measured at days 11 and 14 postsowing. Plants were transferred to rockwool substrate at day 14 postsowing and were examined every 2 d thereafter. Photographs of the plants were taken at key threshold developmental stages. All other plants were treated essentially the same as for the stage-based method, except that seeds were stratified for 7 d. Additionally, photographs of the plants were taken at 14 and 21 DAG rather than at threshold developmental stages.

Plant Data Collection and Image Analysis

Data collection was managed by a Web page-based user interface (Grigor et al., 2003). Digital images of the plants were taken using a Pixera professional digital camera. For floral images, a Pixera professional digital camera mounted on a Leica wild MS5 microscope (Leica Microsystems) with a PLAN 1.0× objective lens was used. Digital image analysis was performed using custom Visual Basic automation and image analysis scripts run within MetaMorph imaging software (Universal Imaging).

Sequence data from this article can be found in the GenBank/EMBL data libraries under accession numbers AY618655, AY618656, AY618657, and AY618658.

ACKNOWLEDGMENTS

We wish to thank Reshma Devi, Simon Harris, Mat Rowe, and Neelam Sharma for their excellent technical assistance in the phenotypic examination of the plants, and Shining Yuan and the members of the AgriGenesis Technology Platforms groups for their work in the cloning, sequencing, and transformation of the gene expression constructs. We are grateful to Alan Moore of Double Design, Auckland, for the development of the Genesis Phenotyping System (GPS) platform used to acquire and manage the data from these and other experiments, and Roger Lainson of SDR Clinical Technologies, Sydney, for the design and creation of the image analysis-GPS interface software. Finally, we thank Richard Forster, Bill Lucas, and Paul Sanders for helpful discussions and/or critical reading of the manuscript.

Received December 16, 2005; revised December 16, 2005; accepted February 4, 2006; published February 17, 2006.

LITERATURE CITED

Alonso JM, Stepanova AN, Leisse TJ, Kim CJ, Chen H, Shinn P, Stevenson DK, Zimmerman J, Barajas P, Cheuk R, et al (2003) Genome-wide insertional mutagenesis of *Arabidopsis thaliana.* Science **301:** 653–657

Altschul SF, Madden TL, Schaffer AA, Zhang J, Zhang Z, Miller W, Lipman DJ (1997) Gapped BLAST and PSI-BLAST: a new generation of protein database search programs. Nucleic Acids Res **25:** 3389–3402

Arabidopsis Genome Initiative (2000) Analysis of the genome sequence of the flowering plant *Arabidopsis thaliana.* Nature **408:** 796–815

Bäurle I, Laux T (2003) Apical meristems: the plant's fountain of youth. Bioessays **25:** 961–970

Bonello JF, Opsahl-Ferstad HG, Perez P, Dumas C, Rogowsky PM (2000) Esr genes show different levels of expression in the same region of maize endosperm. Gene **246:** 219–227

Bonello J-F, Sevilla-Lecoq S, Berne A, Risueno M-C, Dumas C, Rogowsky PM (2002) Esr proteins are secreted by the cells of the embryo surrounding region. J Exp Bot **53:** 1559–1568

Boyes DC, Zayed AM, Ascenzi R, McCaskill AJ, Hoffman NE, Davis KR, Görlach J (2001) Growth stage-based phenotypic analysis of Arabidopsis: a model for high throughput functional genomics in plants. Plant Cell **13:** 1499–1510

Brand U, Fletcher JC, Hobe M, Meyerowitz EM, Simon R (2000) Dependence of stem cell fate in *Arabidopsis* on a feedback loop regulated by *CLV3* activity. Science **289:** 617–619

Butenko MA, Patterson SE, Grini PE, Stenvik G-E, Amundsen SS, Mandal A, Aalen RB (2003) *INFLORESCENCE DEFICIENT IN ABSCISSION* controls floral organ abscission in Arabidopsis and identifies a novel family of putative ligands in plants. Plant Cell **15:** 2296–2307

Carles CC, Fletcher JC (2003) Shoot apical meristem maintenance: the art of a dynamic balance. Trends Plant Sci **8:** 394–401

Casamitjana-Martinez E, Hofhuis HF, Xu J, Liu CM, Heidstra R, Scheres B (2003) Root-specific CLE19 overexpression and the sol1/2 suppressors implicate a CLV-like pathway in the control of *Arabidopsis* root meristem maintenance. Curr Biol **13:** 1435–1441

Clark SE, Running MP, Meyerowitz EM (1995) *CLAVATA3* is a specific regulator of shoot and floral meristem development affecting the same processes as *CLAVATA1.* Development **121:** 2057–2067

Clough SJ, Bent AF (1998) Floral dip: a simplified method for *Agrobacterium*-mediated transformation of *Arabidopsis thaliana.* Plant J **16:** 735–743

Cock JM, McCormick S (2001) A large family of genes that share homology with CLAVATA3. Plant Physiol **126:** 939–942

Diévart A, Dalal M, Tax FE, Lacey AD, Huttly A, Li J, Clark SE (2003) CLAVATA1 dominant-negative alleles reveal functional overlap between multiple receptor kinases that regulate meristem and organ development. Plant Cell **15:** 1198–1211

Doerner P (2003) Plant meristems: a merry-go-round of signals. Curr Biol **13:** R368–R374

Fiers M, Golemiec E, Xu J, van der Geest L, Heidstra R, Stiekema W, Liu C-M (2005) The 14-amino acid CLV3, CLE19, and CLE40 peptides

trigger consumption of the root meristem in Arabidopsis through a CLAVATA2-dependent pathway. Plant Cell **17:** 2542–2553

Fiers M, Hause G, Boutilier K, Casamitjana-Martinez E, Weijers D, Offringa R, van der Geest L, van Lookeren Campagne M, Liu C-M (2004) Mis-expression of the CLV3/ESR-like gene CLE19 in *Arabidopsis* leads to a consumption of root meristem. Gene **327:** 37–49

Fletcher JC, Brand U, Running MP, Simon R, Meyerowitz EM (1999) Signaling of cell fate decisions by *CLAVATA3* in *Arabidopsis* shoot meristems. Science **283:** 1911–1914

Gibeaut DM, Hulett J, Cramer GR, Seemann JR (1997) Maximal biomass of *Arabidopsis thaliana* using a simple, low-maintenance hydroponic method and favorable environmental conditions. Plant Physiol **115:** 317–319

Gleave AP (1992) A versatile binary vector system with a T-DNA organisational structure conducive to efficient integration of cloned DNA into the plant genome. Plant Mol Biol **20:** 1203–1207

Grigor MR, Phillips J, Puthigae S, Strabala TJ (2003) Sequence to systems: a pipeline for gene discovery in forestry. New Zealand Bioscience **12:** 5–7

Haas BJ, Volfovsky N, Town CD, Troukhan M, Alexandrov N, Feldmann KA, Flavell RB, White O, Salzberg SL (2002) Full-length messenger RNA sequences greatly improve genome annotation. Genome Biol **3:** 1–12

Haruta M, Constabel CP (2003) Rapid alkalinization factors in poplar cell cultures. Peptide isolation, cDNA cloning, and differential expression in leaves and methyl jasmonate-treated cells. Plant Physiol **131:** 814–823

Hobe M, Müller R, Grünewald M, Brand U, Simon R (2003) Loss of CLE40, a protein functionally equivalent to the stem cell restricting signal CLV3, enhances root waving in *Arabidopsis*. Dev Genes Evol **213:** 371–381

Kakimoto T (1996) CKI1, a histidine kinase homolog implicated in cytokinin signal transduction. Science **274:** 982–985

Kirch T, Simon R, Grunewald M, Werr W (2003) The *DORNROSCHEN/ENHANCER OF SHOOT REGENERATION1* gene of Arabidopsis acts in the control of meristem cell fate and lateral organ development. Plant Cell **15:** 694–705

Laux T, Mayer KFX, Berger J, Jürgens G (1996) The *WUSCHEL* gene is required for shoot and floral meristem integrity in *Arabidopsis*. Development **122:** 87–96

Lindsey K, Casson S, Chilley P (2002) Peptides: new signalling molecules in plants. Trends Plant Sci **7:** 78–83

Nielsen H, Engelbrecht J, Brunak S, von Heijne G (1997) Identification of prokaryotic and eukaryotic signal peptides and prediction of their cleavage sites. Protein Eng **10:** 1–6

Olsen AN, Mundy J, Skriver K (2002) Peptomics, identification of novel cationic Arabidopsis peptides with conserved sequence motifs. In Silico Biol **2:** 441–451

Olsen AN, Skriver K (2003) Ligand mimicry? Plant-parasitic nematode polypeptide with similarity to CLAVATA3. Trends Plant Sci **8:** 55–57

Page RDM (1996) TreeView: an application to display phylogenetic trees on personal computers. Comput Appl Biosci **12:** 357–358

Pearce G, Moura DS, Stratmann J, Ryan CA Jr (2001) RALF, a 5-kDa ubiquitous polypeptide in plants, arrests root growth and development. Proc Natl Acad Sci USA **98:** 12843–12847

Pearce G, Strydom D, Johnson S, Ryan CA (1991) A polypeptide from tomato leaves induces wound-inducible proteinase inhibitor proteins. Science **253:** 895–898

Rojo E, Sharma VK, Kovaleva V, Raikhel NV, Fletcher JC (2002) CLV3 is localized to the extracellular space, where it activates the Arabidopsis CLAVATA stem cell signaling pathway. Plant Cell **14:** 969–977

Ryan CA, Pearce G (2003) Systemins: a functionally defined family of peptide signals that regulate defensive genes in Solanaceae species. Proc Natl Acad Sci USA **100:** 14577–14580

Sambrook J, Fritsch EF, Maniatis T (1989) Molecular Cloning. A Laboratory Manual, Ed 2. Cold Spring Harbor Laboratory Press, Cold Spring Harbor, NY

Sharma VK, Carles C, Fletcher JC (2003a) Maintenance of stem cell populations in plants. Proc Natl Acad Sci USA **100:** 11823–11829

Sharma VK, Ramirez J, Fletcher JC (2003b) The *Arabidopsis CLV3*-like (*CLE*) genes are expressed in diverse tissues and encode secreted proteins. Plant Mol Biol **51:** 415–425

Shiu S-H, Bleecker AB (2001) Receptor-like kinases from *Arabidopsis* form a monophyletic gene family related to animal receptor kinases. Proc Natl Acad Sci USA **98:** 10763–10768

Shpak ED, Berthiaume CT, Hill EJ, Torii KU (2004) Synergistic interaction of three ERECTA-family receptor-like kinases controls *Arabidopsis* organ growth and flower development by promoting cell proliferation. Development **131:** 1491–1501

Stevenson LF, Kennedy BK, Harlow E (2001) A large-scale overexpression screen in Saccharomyces cerevisiae identifies previously uncharacterized cell cycle genes. Proc Natl Acad Sci USA **98:** 3946–3951

Thompson J, Gibson T, Plewniak F, Jeanmougin F, Higgins D (1997) The CLUSTAL_X windows interface: flexible strategies for multiple sequence alignment aided by quality analysis tools. Nucleic Acids Res **25:** 4876–4882

Vanoosthuyse V, Miege C, Dumas C, Cock JM (2001) Two large *Arabidopsis thaliana* gene families are homologous to the Brassica gene superfamily that encodes pollen coat proteins and the male component of the self-incompatibility response. Plant Mol Biol **46:** 17–34

Wang X, Mitchum MG, Gao B, Li C, Diab H, Baum TJ, Hussey RS, Davis EL (2005) A parasitism gene from a plant-parasitic nematode with function similar to CLAVATA3/ESR (CLE) of *Arabidopsis thaliana*. Mol Plant Pathol **6:** 187–191

Wen J, Lease KA, Walker JC (2004) DVL, a novel class of small polypeptides: overexpression alters *Arabidopsis* development. Plant J **37:** 668–677

Yang H, Matsubayashi Y, Nakamura K, Sakagami Y (2001) Diversity of Arabidopsis genes encoding precursors for phytosulfokine, a peptide growth factor. Plant Physiol **127:** 842–851

Zhang JZ (2003) Overexpression analysis of plant transcription factors. Curr Opin Plant Biol **6:** 430–440